



Contents lists available at ScienceDirect

# Journal of Rock Mechanics and Geotechnical Engineering

journal homepage: [www.jrmge.cn](http://www.jrmge.cn)

Full Length Article

## Improvement of underwater durability and liquefaction evaluation of biopolymer-treated soil using tannic acid



Jeong Youn Lee<sup>a</sup>, Jae-Eun Ryou<sup>a</sup>, Sangbeen Lee<sup>a</sup>, Beomjoo Yang<sup>a</sup>, Chiyoung Park<sup>b</sup>, Jongwon Jung<sup>a,\*</sup>

<sup>a</sup> School of Civil Engineering, Chungbuk National University, 1, Chungdae-ro, Seowon-gu, Chungbuk, Cheongju-si, Chungcheongbuk-do, 28644, South Korea

<sup>b</sup> Department of Energy Science and Engineering, Daegu Gyeongbuk Institute of Science and Technology, 333, Techno Jungang Daero, Hyeonpung-Eup, Dalseong-gun, Daegu, 42988, South Korea

### ARTICLE INFO

#### Article history:

Received 7 November 2024

Received in revised form

21 April 2025

Accepted 15 May 2025

Available online 13 June 2025

#### Keywords:

Biopolymer-treated soils

Underwater stability

Tannic acid

Soil particle bonding

Cyclic simple shear tests

Liquefaction resistance strength

### ABSTRACT

Liquefaction occurs when loose, saturated sandy soils lose strength due to cyclic loads, like earthquakes, causing ground subsidence and structural collapse. While mitigation is possible, conventional cement-based methods have drawbacks, including carbon emissions and groundwater contamination. Consequently, there is a growing emphasis on the need for eco-friendly ground reinforcement materials. Research on biopolymer-treated soils lacks focus on underwater stability and performance degradation. This study used tannic acid to improve underwater durability, as confirmed through soil bonding experiments and cyclic shear tests. The optimal tannic acid formulation, based on gelatin content, enhanced liquefaction resistance and maintained stable strength during underwater curing.

© 2026 Institute of Rock and Soil Mechanics, Chinese Academy of Sciences. Published by Elsevier B.V. This is an open access article under the CC BY-NC-ND license (<http://creativecommons.org/licenses/by-nc-nd/4.0/>).

## 1. Introduction

Soil liquefaction primarily occurs in loose, saturated sandy soils when dynamic loads, such as those from earthquakes, are applied. This phenomenon is driven by an increase in excess pore water pressure due to dynamic loading, which reduces effective stress and causes a loss of soil stiffness and shear strength (Owen, 1987). As a result, the soil behaves like a liquid, potentially leading to damage from soil liquefaction during an earthquake. Preventing and predicting liquefaction, as well as analyzing volumetric deformation, are crucial tasks in geotechnical engineering (Alshawmar and Fall 2021; Nagula et al., 2021; Ray and Sahu, 2021; Do et al., 2023).

In 2017, South Korea experienced its first recorded instance of soil liquefaction following a 5.4 magnitude earthquake in Pohang (Gihm et al., 2018; Park et al., 2018; Naik et al., 2020; Ji et al., 2021; Kim et al., 2021). Consequently, around 100 locations within a

2 km radius of the epicenter showed signs of muddy water ejection, and many buildings, including tilted apartment complexes in Pohang, sustained damage due to liquefaction. This event underscores the necessity of ground reinforcement. However, conventional cement-based reinforcement methods, such as cement grouting, compaction grout, and the free-jet grout technique, pose substantial environmental concerns. These issues include soil alkalization, elevated pH levels in nearby groundwater, and increased carbon dioxide emissions (Worrell et al., 2001; Chang et al., 2020; Zivari, A et al., 2023; Sierra, K et al., 2024). These factors contribute to abnormal climate phenomena, such as urban heat islands, which are associated with a rise in geotechnical hazards such as heavy rainfall, landslides, ground subsidence, and river flooding (Schuster and Fleming, 1986; Galloway et al., 1999; Sato et al., 2006; Teatini et al., 2006; Wang and Li, 2009; Jang et al., 2024). Thus, the necessity for eco-friendly ground reinforcement materials that can enhance ground stability while minimizing environmental impact has become increasingly urgent. This study aims to evaluate the effectiveness of using eco-friendly biopolymers for ground reinforcement.

Biopolymers are polymers derived from living organisms and can be classified based on their physical properties into water-

\* Corresponding author.

E-mail address: [jjung@chungbuk.ac.kr](mailto:jjung@chungbuk.ac.kr) (J. Jung).

Peer review under responsibility of Institute of Rock and Soil Mechanics, Chinese Academy of Sciences.

soluble and thermo-gelation types. Water-soluble biopolymers dissolve in water, whereas thermo-gelation biopolymers, such as gelatin and agar gum, undergo phase changes with temperature. Common biopolymers used for soil strengthening include xanthan gum, guar gum, agar gum, gelatin, sodium alginate, carrageenan, chitosan, and casein. These biopolymers improve soil strength by forming interlocking structures and biopolymer gels within soil pores. They are renewable, sustainable, and eco-friendly (Ryou et al., 2024a, 2024b). Various studies have investigated their use as ground reinforcement materials, taking into account different soil types and curing methods. Previous research on biopolymer applications can be broadly categorized as follows.

The strength characteristics of soils treated with biopolymers have been examined. Experiments were conducted to evaluate the performance of biopolymer reinforcement as an alternative to conventional cement-based methods. The unconfined compressive strength of cement-treated soils was compared with that of soils treated with gellan gum and xanthan gum under dry-curing conditions. The results confirmed that biopolymer-based ground reinforcement offers superior strength compared to conventional cement-based materials, highlighting its effectiveness as a viable alternative (Chang et al., 2015a, 2020).

Studies have investigated the grouting injectability of biopolymers. Previous research has evaluated the effectiveness of biopolymers as grouting injection materials. The biopolymers used in the experiments were agar and gellan gum. The physical properties of the biopolymer solutions, including viscosity, interfacial tension, and surface contact angle, were assessed to understand their impact on fluid flow. The experimental results showed that the biopolymer solutions exhibited higher viscosity and contact angles compared to water, and their lower interfacial tension created favorable conditions for pore injection. In comparison to conventional injection materials, biopolymer solutions demonstrated superior injectability and workability, indicating their potential for high injection efficiency as permeation grouting materials (Ryou and Jung, 2022, 2023).

Studies have explored the impact of biopolymers on enhancing liquefaction resistance. To investigate various geotechnical applications, liquefaction assessments were conducted on soils treated with biopolymers. The experiments used agar gum, and strain-controlled undrained cyclic triaxial tests demonstrated a lesser increase in pore water pressure in biopolymer-treated soils compared to that in untreated soils (Chang et al., 2015b; Smitha and Rangaswamy, 2020, 2021, 2022a, 2022b). Additionally, cyclic triaxial tests with axial load control showed that biopolymers enhanced liquefaction resistance (Jang et al., 2024, 2025).

Research has also focused on the characteristics of biopolymers under different curing conditions, examining the physical properties of biopolymer-treated soils across various curing techniques. Studies have analyzed the effects on mechanical strength and the relationship between strength and moisture content. For soils treated with agar gum under wet curing conditions, strength and liquefaction resistance were evaluated. Drop cone test results showed minimal variation in strength with curing time, while cyclic triaxial tests under axial load control indicated no significant change in liquefaction resistance with curing duration. These findings suggest that under wet curing, the moisture content and strength of biopolymer-treated soils remain largely stable (Jang et al., 2024). By contrast, for soils under dry curing, strength increased as moisture content decreased (Chen et al., 2019, 2022a; Chang et al., 2020; Fatehi et al., 2023). This phenomenon was attributed to the maximum contraction of the polymer network after drying, which enhanced the strength of the soil particles (Ryou et al., 2024a).

Furthermore, a study was conducted to evaluate the durability of biopolymer-treated soil under cyclic wetting and drying processes. Previous experiments on two soil types treated with xanthan gum and guar gum revealed that repeated wetting and drying cycles reactivated the biopolymer's bonding properties, restoring broken bonds in the soil. These results demonstrate that biopolymer-treated soil is a viable option for rapid temporary structures or long-term constructions in arid climates (Soldo and Miletic, 2022).

Methods for improving the performance of biotreated soil have been studied. Microbially induced carbonate precipitation (MICP) is a new cementation technology that improves the performance of bio-treated soils through interparticle bonding. Particle-level tensile experiments on quartz sand and glass beads showed that increased cementation level and reduced particle shape regularity increased the tensile strength of the MICP bond. As the strength and particle size increase, the tensile strength decreases (Xiao et al., 2024a, 2024b). These studies provide a constitutive model and data for predicting deformation and failure of field-scale biotreated soils.

The performance of biopolymer-based ground reinforcement has been verified through various indoor experiments, and based on these results, the feasibility of field application is being continuously assessed. Recently, practical approaches to expand the applicability of biopolymer materials from laboratory to field scale have been proposed. Biopolymers based on xanthan gum, starch, and  $\beta$ -glucan were applied in the field to improve the structural strength of slopes. By mixing biopolymer binders with in-situ soil and spraying them onto slopes, researchers confirmed that a strength comparable to that achieved under laboratory conditions could be attained (Seo et al., 2021). These findings demonstrate that the field applicability of biopolymers is gradually being validated, though further field experiments will be necessary in the future.

However, limitations were observed for biopolymer-treated soils under underwater curing, where water absorption led to the formation of hydrogels, reducing biopolymer–soil interaction and degrading mechanical performance (Yakimets et al., 2007; Chen et al., 2019, 2022a; Ryou et al., 2024a). Consequently, further research is needed to improve the underwater stability and liquefaction resistance of biopolymer-treated soils.

In this study, the biopolymer tannic acid was used to enhance the water resistance and liquefaction resistance of biopolymer-treated soil submerged in water. The polymer mixed with tannic acid is a biopolymer that reinforces soil through gelation with gelatin (Kozlov and Burdygina, 1983). A slake test was conducted to evaluate the stability of soil treated with the gelatin–tannic acid mixture under underwater curing conditions, with a focus on its underwater cohesion and long-term durability. The optimal mixing ratio was determined by experimentally analyzing soil particle bonding and assessing the shear strength of the gelatin–tannic acid mixture. Furthermore, a cyclic simple shear test was performed to examine the liquefaction resistance of the treated soil under underwater conditions.

## 2. Material and methods

### 2.1. Soils

The soil samples in this study were prepared based on the particle size distribution of soil collected from Songdo-dong, Pohang-si, Gyeongsangbuk-do, South Korea, where Korea's first liquefaction event occurred following a 5.4 magnitude earthquake in 2017 (Hwang et al., 2020). The samples consisted of dry and

washed 4.55% weathered granite, 94.2% silica, and 1.25% kaolinite. According to the Unified Soil Classification System (Stevens, 1982), these samples were classified as clean sand (SP) and exhibited a particle size distribution that made them particularly vulnerable to liquefaction (Iwasaki, 1986). Fig. 1 shows the particle size distribution curve for the soil samples used in the experiment. The region marked within black lines (A) represents the particle size distribution range where liquefaction can occur very easily, and the region marked between the black and red lines (B) represents the particle size distribution range where liquefaction is likely to occur relatively easily. Table 1 summarizes the basic physical properties of the reproduced Pohang soil sample.

2.2. Biopolymer

2.2.1. Gelatin

Gelatin is a colorless to pale-yellow powder or crystal, defined by the United States Pharmacopeia (USP, 1990) (Poppe, 1992) as a product obtained by partially hydrolyzing collagen derived from animal skin, white connective tissue, and bones. Fig. 2 illustrates the chemical structure of gelatin. As a typical rigid-chain polymer, gelatin shares many properties with rigid-chain synthetic polymers, exhibiting general characteristics common to polymer materials. However, similar to linear-chain synthetic polymers, gelatin adopts a coiled structure in aqueous solutions at elevated temperatures. In gelatin films cast at or below room temperature, macromolecules primarily take on a helical structure similar to that of collagen. Experimental evidence indicates that coiled gelatin has lower strength and elasticity compared to its helical forms. Consequently, gelatin can transition from a coiled to a helical structure depending on temperature, and this gelation phenomenon is anticipated to enhance soil performance when utilizing gelatin (Kozlov and Burdygina, 1983).

2.2.2. Tannic acid

Tannic acid is a type of naturally occurring polyphenolic compound derived from the bark, wood, fruit, and leaves of plants. Tannic acid is a natural polyphenolic compound known for its

**Table 1**  
Physical properties of the soil.

$G_s$	$D_{60}$ (mm)	$D_{30}$ (mm)	$D_{10}$ (mm)	$C_u$	$C_c$
2.66	0.22	0.15	0.12	1.83	0.85

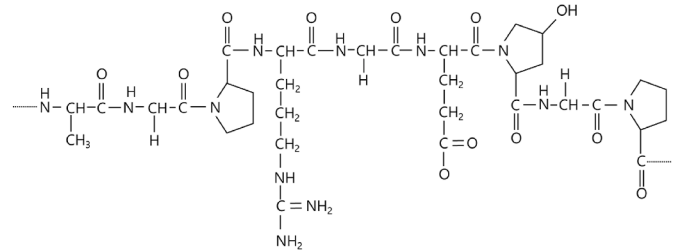


Fig. 2. Chemical structure of gelatin (González et al., 2020).

strong adhesive properties, especially in underwater applications. This adhesive capability stems from its ability to form robust hydrogen bonds with various surfaces, facilitated by its catechol or pyrogallol groups. These interactions can create secondary or triple cross-links that are significantly stronger than single hydrogen bonds, allowing for adaptable adhesion even in aquatic environments (Chen et al., 2022b). Tannic acid contains numerous phenyl groups that enable the formation of hydrogen bonds with various molecules containing carboxyl groups, hydroxyl groups, amino groups, ether linkages, fluorine atoms, nitrogen-containing heterocycles, sulfonates, or phosphates. It appears as a colorless or pale-yellow solid derived from the bark, wood, and leaves of various plants. Tannic acid is inexpensive, environmentally friendly, and biocompatible, highlighting its substantial potential as a smart biomaterial for various engineering applications (Jafari et al., 2022). Additionally, tannic acid can act as a natural inhibitor of microbial populations, effectively suppressing the growth of aquatic microorganisms (Chung et al., 1995). Fig. 3 illustrates the chemical structure of tannic acid.

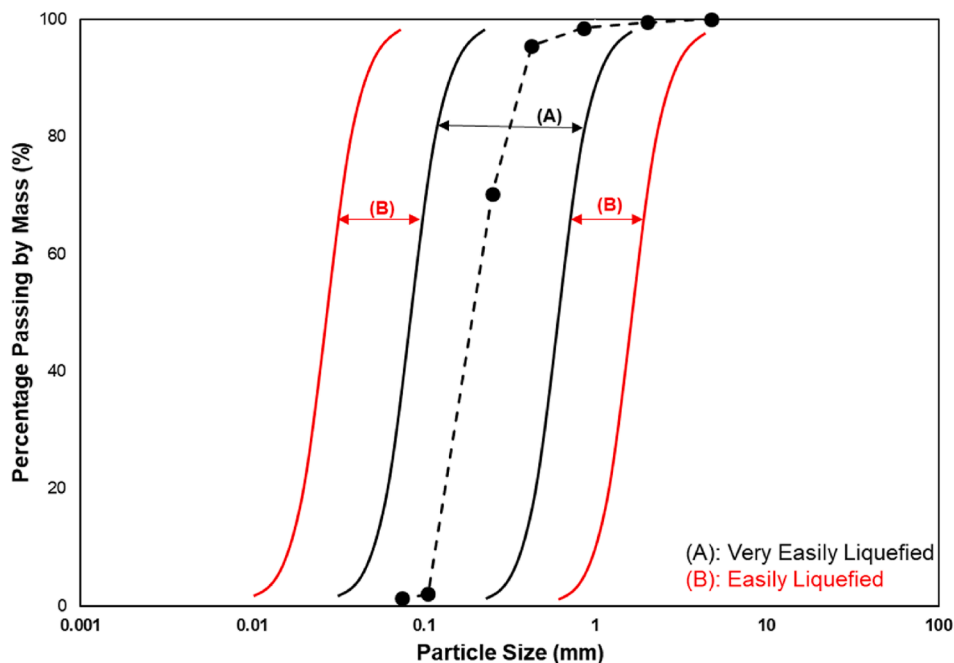


Fig. 1. Particle-size distribution curve with liquefiable boundary (Iwasaki, 1986).

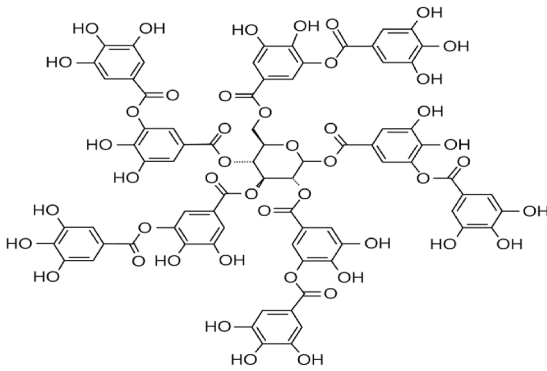


Fig. 3. Chemical structure of tannic acid (Chen et al., 2022b).

2.3. Underwater durability index based on slake test

In this study, a slake test was performed to assess the underwater durability of soil treated with gelatin and tannic acid after underwater curing. The slake test followed the methodology outlined in Park’s study (Park and Hwang, 2012). Table 2 presents the mixing ratios of gelatin and tannic acid used in the tests. The gelatin solution was prepared at 70 °C, whereas the tannic acid solution was prepared at room temperature. To maintain uniformity, the relative density of the reproduced Pohang sample was kept constant at 50% for all mixing ratios. The soil samples were molded into specimens with a diameter of 50 mm and a height of 20 mm, achieving a dry unit weight of 13.43 kN/m<sup>3</sup>.

For the gelatin–tannic acid-treated samples and the gelatin-only-treated samples, dried soil was mixed with a 25% aqueous polymer solution. In the gelatin–tannic acid treatment, the gelatin aqueous solution was first blended with the soil, followed by the addition of the tannic acid aqueous solution. The ratio of the aqueous gelatin solution to the aqueous tannic acid solution was fixed at 1:1. Both the gelatin-treated and gelatin–tannic acid-treated soils underwent underwater curing after an initial 7-d dry curing period, with underwater curing durations of 1 d, 7 d, and 28 d.

The slake test was conducted at 20 RPM for 10 min using a magnetic stirrer and bar, after which the underwater durability index was calculated. Fig. 4 presents a schematic of the slake test. The underwater durability index was determined by dividing the weight of the sample dried after the experiment by the total weight, which is the sum of the weights of the lost sample after drying and the weight of the sample after drying.

Table 2

Slake test details according to the gelatin–tannic acid mixing ratio of the samples.

Curing	$W_{soil}/W_s$	Concentration (%) (Gelatin/Tannic acid)	Concentration (%) (Gelatin)
Submerged curing	25	5/5	5
		5/10	
		5/15	
		10/5	10
		10/10	
		10/15	
		15/5	15
		15/10	
		15/15	
		20/5	20
		20/10	
		20/15	

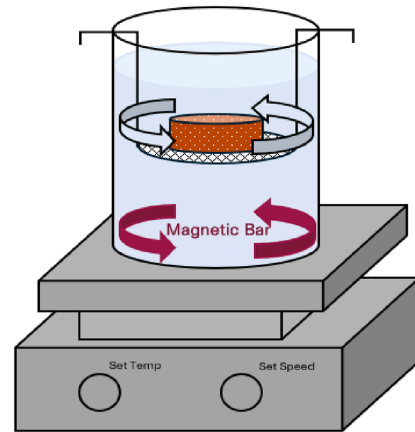


Fig. 4. Schematic of slake test equipment.

2.4. Shear strength based on particle bonding test considering shearing

In this study, soil-particle bonding experiments were conducted to evaluate shear strength by blending soil with gelatin and tannic acid to determine the optimal mixing ratio. The shear experiments utilized equipment comprising silica glass with a diameter of 10 mm, representing silica soil particles, and a cantilever beam with a thickness of 0.5 mm. Four strain gauges were attached to the cantilever beam, and strain data were collected using an oscilloscope with a 9 V electric signal. The device is a self-designed laboratory equipment where shear experiments are performed by placing the polymer between two horizontally separated pieces of silica glass (Lee et al., 2025). A micrometer connected to the upper silica glass is used to move it in the horizontal direction and apply shear displacement. In this process, the shear strength of the polymer is calculated by measuring the strain of the cantilever beam connected to the lower silica glass. To minimize errors during the experiment, calibration was performed to calculate strength in relation to constant voltage changes (strain). Additionally, to prevent strength error during testing, the experiments were conducted at a constant speed of 0.05 mm/s using a micrometer. Fig. 5 displays a schematic of the shear experiment alongside a photograph of the experimental setup.

The gelatin–tannic acid composite polymer was produced by mixing a gelatin aqueous solution and a tannic acid aqueous solution in a 1:1 ratio. The weight used in the experiment was set at 200 mg, which was sufficient to cover the entire glass surface. Fig. 6 illustrates the application of the gelatin–tannic acid mixed polymer on the glass. The experiment was conducted with a drying–curing time of 1 h. Table 3 presents the mixing ratios of the gelatin–tannic acid polymer that were subjected to the shear test.

2.5. Liquefaction resistance strength based on cyclic simple shear tests

In this study, the liquefaction resistance strength of gelatin–tannic acid-treated soil after underwater curing was evaluated by determining the cyclic resistance ratio (CRR) through stress-controlled cyclic shear tests. The composition of the gelatin–tannic acid-treated soil matched that of the slake test sample, with specimens molded to a diameter of 70 mm and height of 17 mm (ASTM-D8296-19). Similar to the slake test, the treated soil underwent 7 d of dry curing followed by underwater curing periods of 1 d, 7 d, and 28 d. Table 4 summarizes the cyclic shear test

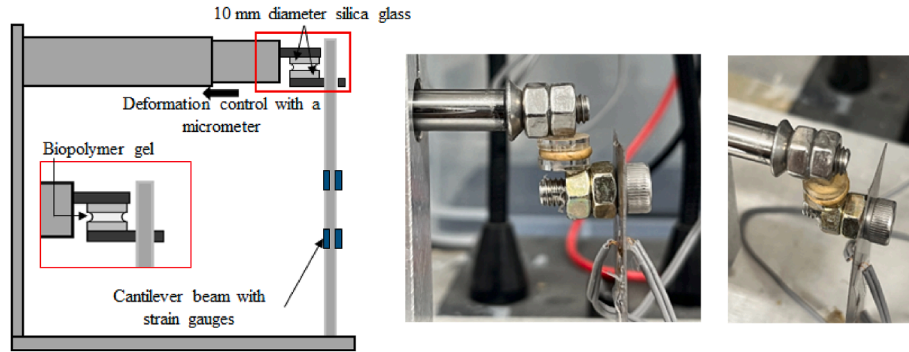


Fig. 5. Schematic of shear test equipment.

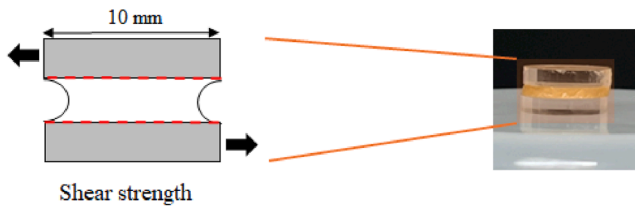


Fig. 6. Gelatin-tannic acid composite polymer coated on silica glass.

Table 3  
Shear test details according to gelatin-tannic acid mixing ratio.

Curing	Curing time (h)	Concentration ( $W_{pol}/W_{sol}$ ) (%) (Gelatin/Tannic acid)
Dry	1	5/5
		5/10
		5/15
		5/20
		10/5
		10/10
		10/15
		10/20
		15/5
		15/10
		15/15
		15/20
		20/5
		20/10
20/15		
20/20		

conditions. The experiments were conducted using a cyclic shear device (GDS Electromechanical Dynamic Cyclic Simple Shear Device, GDS INSTRUMENT, UK), an NGI-type apparatus. The testing sequence included sample installation, docking, consolidation, and cyclic shear stress loading. First, the molded specimen was placed in a mold with tightly sealed membranes and Teflon-coated rings using a vacuum pump. A light vertical load was applied for initial docking to ensure no sample deformation. Docking refers to connecting the sample to the top cap, followed by combining the membrane with the top cap with the application of a weak vertical load. Preconsolidation was performed after docking. After preconsolidation, the sample was consolidated under vertical stresses of 12 kPa, 25 kPa, 50 kPa, and 100 kPa until vertical strain stabilized under the 100 kPa load. While consolidation can be adjusted for specific liquefaction conditions, a 100 kPa load was used as the standard. Once consolidated, an undrained cyclic shear test was conducted by applying a sinusoidal cyclic shear stress. The test maintained constant volume conditions, preventing any volume change. A stress frequency of 0.1 Hz ensured stable stress

Table 4  
Experimental conditions of the cyclic simple shear test.

Polymer	Curing	Concentration (%)	Curing time (d)	Cyclic Stress Ratio (CSR)		
Gel + Tan	Submerged curing	Gel 5 + Tan 15	1	0.15		
				0.2		
		7	0.25			
			0.15			
		28	0.2			
			0.25			
						0.15
						0.2
						0.25

Note: Gel refers to Gelatin, and Tan refers to Tannic acid.

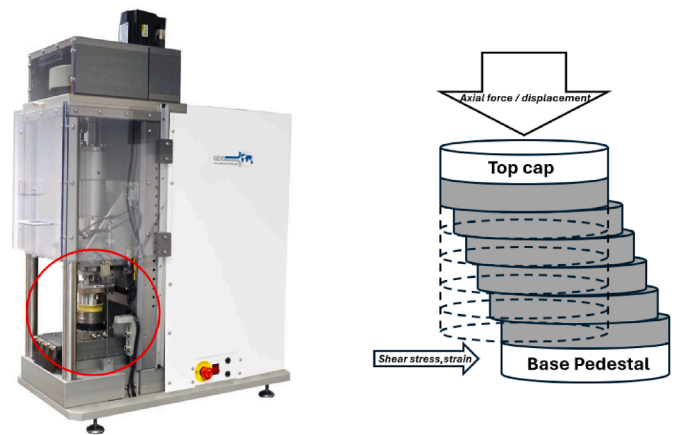


Fig. 7. Cyclic shear test equipment.

application (Nong et al., 2021). The test was terminated when shear strain exceeded 7.5% (Vaid and Sivathayalan, 1996). To determine the cyclic resistance stress ratio, more than three tests with varying cyclic shear stresses were required. Thus, three identical specimens were prepared and tested under different shear stresses to calculate the CRR. Fig. 7 shows the cyclic shear test equipment and experimental setup.

### 3. Experimental results and analysis

#### 3.1. Reaction between gelatin and tannic acid

##### 3.1.1. Chemical reaction between gelatin and tannic acid

Large gelatin molecules absorb water through their polar groups, forming strong hydrogen bonds with water, which results in high hydrophilicity (Chen et al., 2022b).

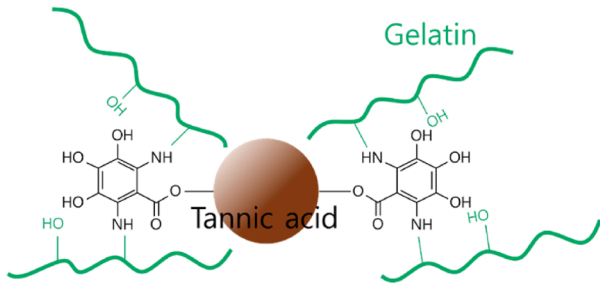


Fig. 8. Hydrogen bonding between tannic acid and gelatin.

Tannic acid can form secondary bonds or triple cross-links through hydrogen bonding with molecules containing hydroxyl and amino groups (Jafari et al., 2022). Gelatin's molecular formula includes a hydroxyl group (–OH) and an amino group (–NH<sub>2</sub>), indicating that tannic acid and gelatin can establish secondary bonds or triple cross-links through hydrogen bonding. These bonds enhance the material's structural integrity, improving its mechanical properties and stability (Kozlov and Burdygina, 1983). Fig. 8 illustrates the chemical structures of tannic acid and gelatin after hydrogen bonding. Consequently, the hydrolytic dissociation of gelatin is improved by preventing the hydrogen bonding of gelatin molecules with water, owing to the prior hydrogen bonding between gelatin and tannic acid.

3.1.2. Analysis of reaction between gelatin and tannic acid

To analyze the mechanism of soil strength enhancement through hydrogen bonding between gelatin and tannic acid, scanning electron microscopy (SEM) experiments were conducted. Fig. 9a and c presents the original SEM images, while Fig. 9b and d is zoomed-in sections of the red-marked regions in Fig. 9a and c to closely examine the polymer networks formed by hydrogen bonding between gelatin and tannic acid and their interactions with soil particles. From Fig. 9b and d, it is evident that the polymer networks, formed via hydrogen bonding between gelatin and tannic acid, coat the soil particles. These coated polymer networks interconnect, effectively filling the micro-voids between soil particles and binding them strongly, thereby contributing to the enhancement of soil strength.

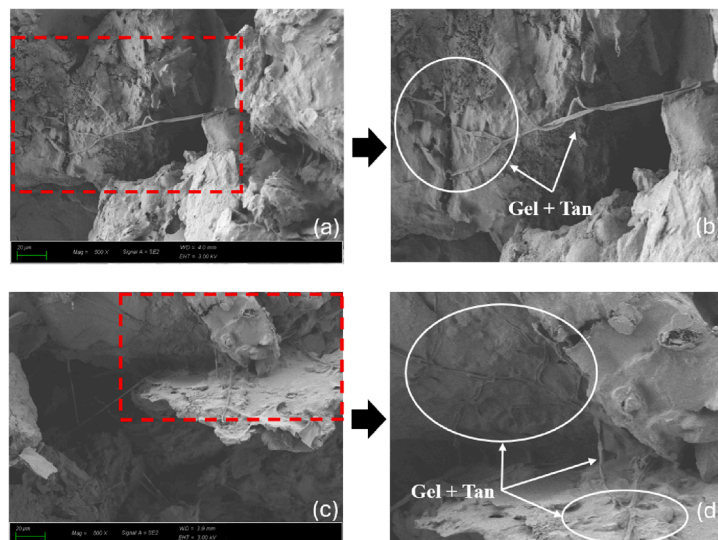


Fig. 9. SEM images of reaction between gelatin and tannic acid.

3.2. Slake test (underwater durability index)

3.2.1. Results of slake test (underwater durability index)

The underwater durability index was calculated using Eq. (1) (Park and Hwang, 2012). For clarity in representing the mixing ratio of the treated soil, gelatin is abbreviated as G and tannic acid as T. The results of the slake test are shown in Fig. 10.

$$\text{Durability index} = \left\{ \frac{W_{\text{Dried Sample after the experiment}}}{W_{\text{Dried sample after the experiment}} + W_{\text{Dried lost sample after the experiment}}} \right\} \times 100 \quad (1)$$

From Fig. 10a, it is evident that G5T10 (gelatin 5%+tannic acid 10%), G5T15 (gelatin 5%+tannic acid 15%) maintained a 100% underwater durability index until 28 d of underwater curing. G5T5 also maintained a 100% underwater durability index for 14 d, with a slight decrease to 99.76% by the 28 d of underwater curing. However, all G5-treated soil samples disintegrated in water on the first day of underwater curing.

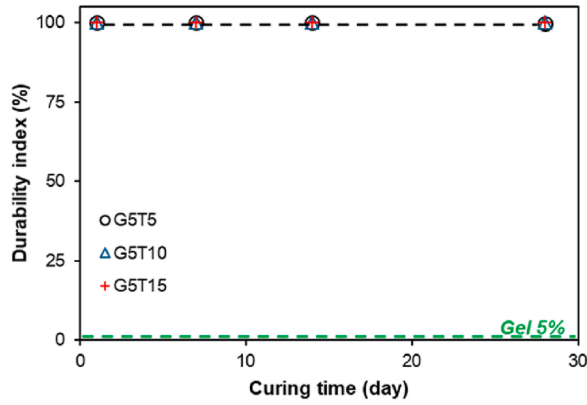
Fig. 10b shows that G10T5, G10T10, G10T15 maintained an underwater durability index of 100% until 28 d of underwater curing. However, the G10-treated soil sample completely dissolved in water after 1 d of underwater curing.

Fig. 10c shows that G15T5, G15T10, G15T15 samples maintained an underwater durability index of 100% until 14 d of underwater curing. After 28 d, the underwater durability indices for G15T5, G15T10, and G15T15 were 99.77%, 99.77%, and 99.88%, respectively, indicating durability indices close to 100%. The G15-treated soil exhibited an underwater durability of 88.6% after 1 d of underwater curing, but was completely dissolved in water after 2 d.

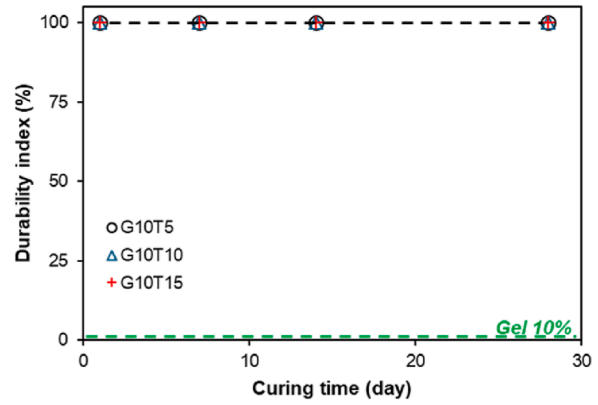
Fig. 10d shows that G20T5, G20T10, G20T15 maintained an underwater durability index of 100%, while after 28 d of underwater curing, the underwater durability indices were 49.15% for G20T5, 100% for G20T10, and 99.01% for G20T15. The G20-treated soil demonstrated an underwater durability of 97.25% after 1 d of underwater curing and 86.63% after 2 d; however, all samples dissolved in water after 3 d of underwater curing.

3.2.2. Analysis of slake test (underwater durability index) analysis

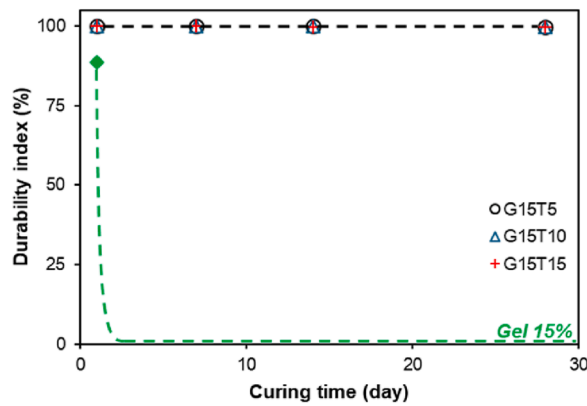
Theoretically, gelatin molecules form strong hydrogen bonds with water through their polar groups, resulting in high hydrophilicity. Based on this mechanism, the slake test results indicated that soils treated with 5%, 10%, 15%, and 20% gelatin decomposed



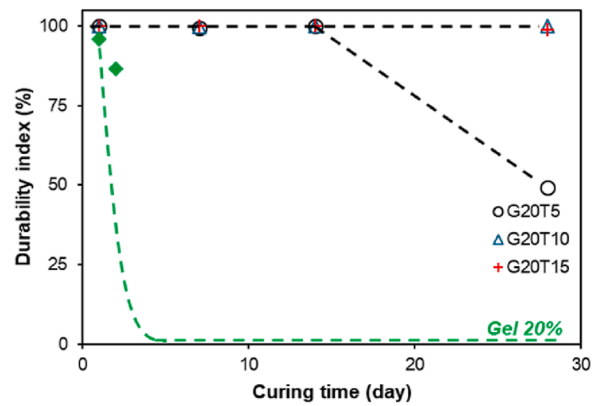
(a)



(b)



(c)



(d)

Fig. 10. Durability index according to days of submerge curing.

completely within 3 d of underwater curing. Theoretically, hydrogen bonding between tannic acid and gelatin inhibits the hydrogen bonding of gelatin molecules with water, thereby enhancing the water resistance of gelatin. Based on this mechanism, the results from the slake tests indicated that the gelatin–tannic acid–treated soil demonstrated an underwater durability index close to 100% for all mixing ratios, except for G20T5, over a 28-d underwater curing period. This finding confirms that the hydrogen bonds between gelatin and tannic acid were stably maintained even during underwater curing. Fig. 11 presents the underwater durability index based on the mixing ratio after 28 d of underwater curing. During the mixing process of the 20% gelatin aqueous solution with the tannic acid aqueous solution, achieving a smooth blend was challenging owing to the high viscosity of the 20% gelatin solution. This difficulty influenced the underwater durability index of G20T5 after 28 d of underwater curing.

Fig. 12 displays the experimental slake samples subjected to underwater curing. The left photograph shows the samples on the 3rd day of underwater curing for soil treated with 15% and 20% gelatin, while the right photograph shows the status on the 28th day of underwater curing for soil treated with 10% and 15% tannic acid, according to the gelatin content. As observed in the experimental results, the gelatin-treated soil was completely dissolved within 3 d of underwater curing, whereas the soil treated with 10%

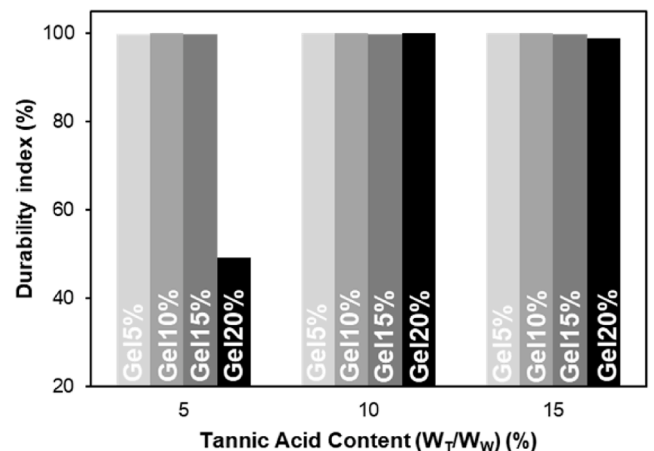


Fig. 11. Underwater durability index on the 28th day of underwater curing.

and 15% tannic acid exhibited no deformation even after 28 d of underwater curing. Fig. 13 depicts the interaction of gelatin and water among soil particles, while Fig. 14 illustrates the reaction between gelatin and tannic acid with water, resulting in hydrogen bond formation among the soil particles.

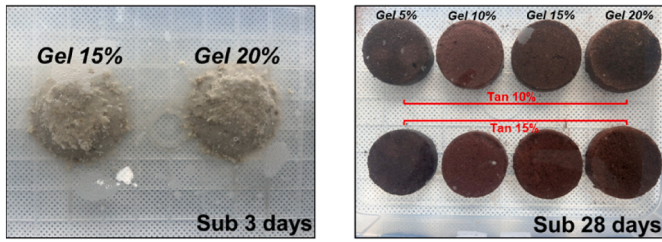


Fig. 12. Photographs of slake test samples subjected to underwater curing.

3.3. Particle bonding test considering shearing (shear strength)

3.3.1. Results of particle bonding test considering shearing (shear strength)

The optimum mixing ratio for each gelatin content was confirmed through soil particle bonding experiments considering

shearing. Fig. 15 displays the raw data from the shear experiments for the G10T5, G10T10, G10T15, and G10 T20 mixing ratios. The strength was calculated by calibrating the bolt change (strain) obtained from the strain gauge attached to the cantilever beam using an oscilloscope.

Experimental results from Fig. 16a show the shear strength results for 5%, 10%, 15%, and 20% tannic acid with 5% gelatin; 5% tannic acid produced a strength of 1.68 kPa, 10% yielded 2.98 kPa, 15% reached 4.87 kPa, and 20% resulted in 2.88 kPa. As the tannic acid concentration increased from 5% to 15%, the shear strength also increased; however, it decreased at 20% concentration.

Experimental results from Fig. 16b present the shear strength results for 5%, 10%, 15%, and 20% tannic acid with 10% gelatin. The findings indicate that 5% tannic acid achieved a strength of 1.98 kPa, 10% produced 3.49 kPa, 15% reached 4.64 kPa, and 20% resulted in 3.38 kPa. Similar to the previous experiment, the shear strength increased from 5% to 15%, but decreased at 20% concentration.

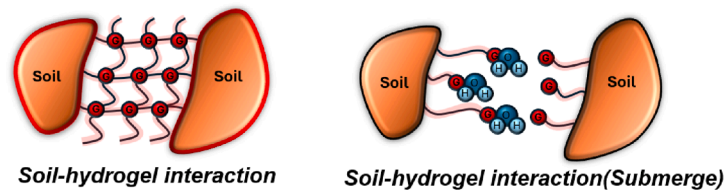


Fig. 13. Reaction between gelatin and water among soil particles.

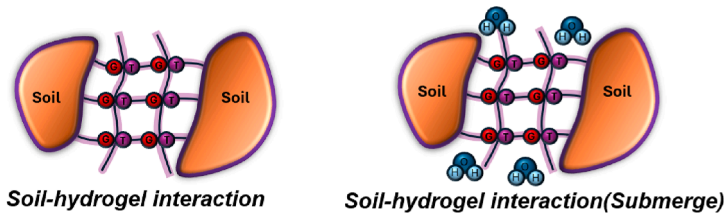


Fig. 14. Interaction between gelatin, tannic acid, and water, forming hydrogen bonds between soil particles.

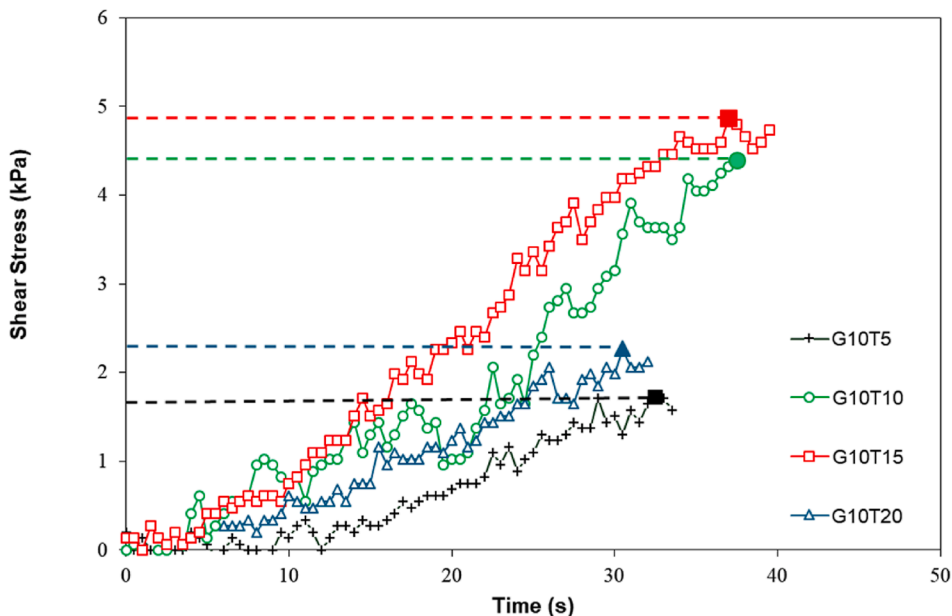


Fig. 15. Shear strength raw data for G10T5, G10T10, G10T15, G10T20.

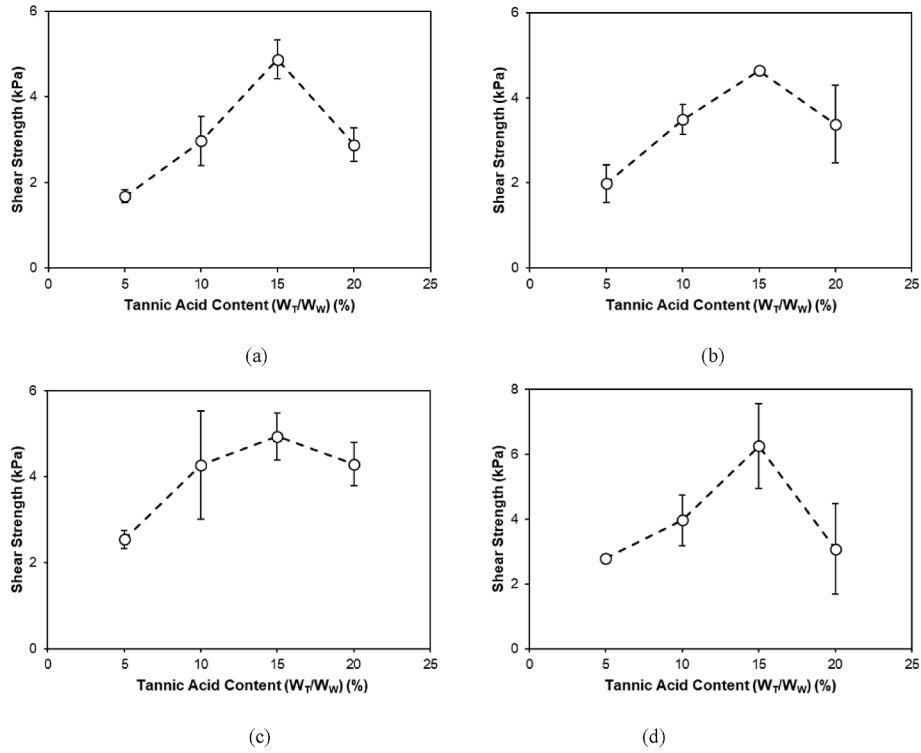


Fig. 16. Shear strength of gelatin-tannic acid mixture.

Experimental results from Fig. 16c illustrate the shear strength results for 5%, 10%, 15%, and 20% tannic acid with 15% gelatin. The experiment showed that 5% tannic acid provided a strength of 2.54 kPa, 10% yielded 4.27 kPa, 15% reached 4.93 kPa, and 20% resulted in 4.29 kPa. The shear strength increased as the tannic acid concentration increased from 5% to 15%, followed by a decrease at 20% concentration.

Experimental results from Fig. 16d demonstrate the shear strength results for 5%, 10%, 15%, and 20% tannic acid with 20% gelatin. The findings revealed that 5% tannic acid produced a strength of 2.79 kPa, 10% yielded 3.96 kPa, 15% reached 6.24 kPa, and 20% resulted in 3.07 kPa. As with the previous experiments, the shear strength increased as tannic acid concentration increased from 5% to 15%, but decreased at 20% concentration.

### 3.3.2. Particle bonding test considering shearing (shear strength) analysis

The results of the slake test showed that all mixing ratios except for G20T5 maintained an underwater durability index close to 100% over 28 d of underwater curing. Consequently, the slake test alone has limitations in determining the optimal mixing ratio of gelatin-tannic acid. Therefore, the optimal mixing ratio for each gelatin content was established through a soil-particle bonding test that considered shearing. Evaluation of the shear strength of the gelatin-tannic acid mixed polymer confirmed that a 15% tannic acid mixing ratio was optimal for gelatin contents of 5%, 10%, 15%, and 20%. Fig. 17 presents the results of the shear test, indicating that strength increased with tannic acid content up to 15%; however, at 20% tannic acid, the strength decreased for all gelatin contents. This suggests that the effective ratio for enhancing mechanical strength through hydrogen bonds formed when tannic acid is combined with gelatin is most appropriate at 15%. As observed in the experimental results, the addition of more than 20% tannic acid leads to a decrease in bond stability.

### 3.4. Cyclic simple shear tests (CRR)

#### 3.4.1. Results of cyclic simple shear tests (CRR)

The liquefaction resistance strength of the samples was assessed by calculating CRR using CSR, derived from stress-controlled cyclic shear tests conducted on both biopolymer-treated and untreated soils. The equation for calculating the cyclic shear stress ratio is (ASTM D8296 – 19):

$$CSR = \frac{\tau_{cyc}}{\sigma_{vc}}, \tau_{cyc} = \frac{\tau_{max} - \tau_{min}}{2} \tag{2}$$

where  $\tau_{max}$  denotes the maximum shear stress during a given cycle,  $\tau_{min}$  denotes the minimum shear stress during a given cycle, and  $\sigma_{vc}$  denotes the vertical axial stress at the end of the last consolidation stage. To calculate CRR, a sample subjected to consistent conditions underwent three repeated shear tests to establish a liquefaction resistance curve. The CRR was then determined using this derived curve. Specifically, the CRR was identified by locating the point on the liquefaction resistance curve after 15 cycles of repeated loading, corresponding to an earthquake magnitude of 7.5, which serves as the standard for international liquefaction evaluation (Bolton Seed et al., 1985).

The optimal gelatin-tannic acid mixing ratio was established through slake and shear tests. The experimental results confirmed that hydrogen bonding, dependent on the ratio of gelatin to tannic acid, plays a crucial role in maintaining mechanical strength and underwater durability. As the 15% tannic acid ratio yielded the most effective results among the mixing ratios for varying gelatin content, it can be proposed as the optimal mixing ratio for gelatin-tannic acid hydrogen bonding. To demonstrate the effective enhancement of underwater liquefaction resistance strength even with the lowest polymer content, G5T15 was selected from the gelatin-tannic acid blending ratios, considering the economic feasibility of using 15% tannic acid. The gelatin-tannic acid-treated

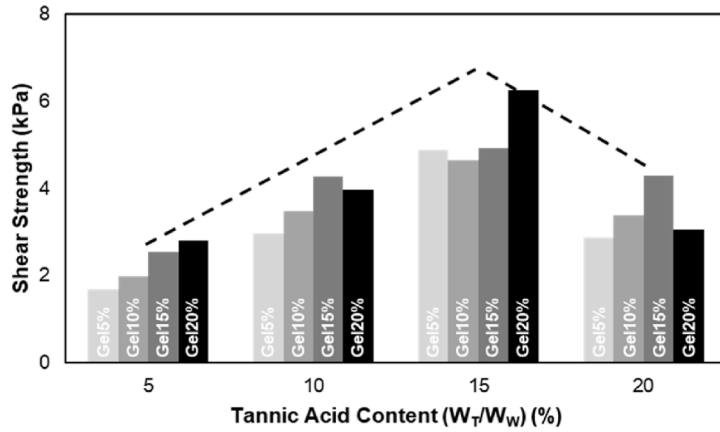


Fig. 17. Shear strength of gelatin–tannic acid self-polymer.

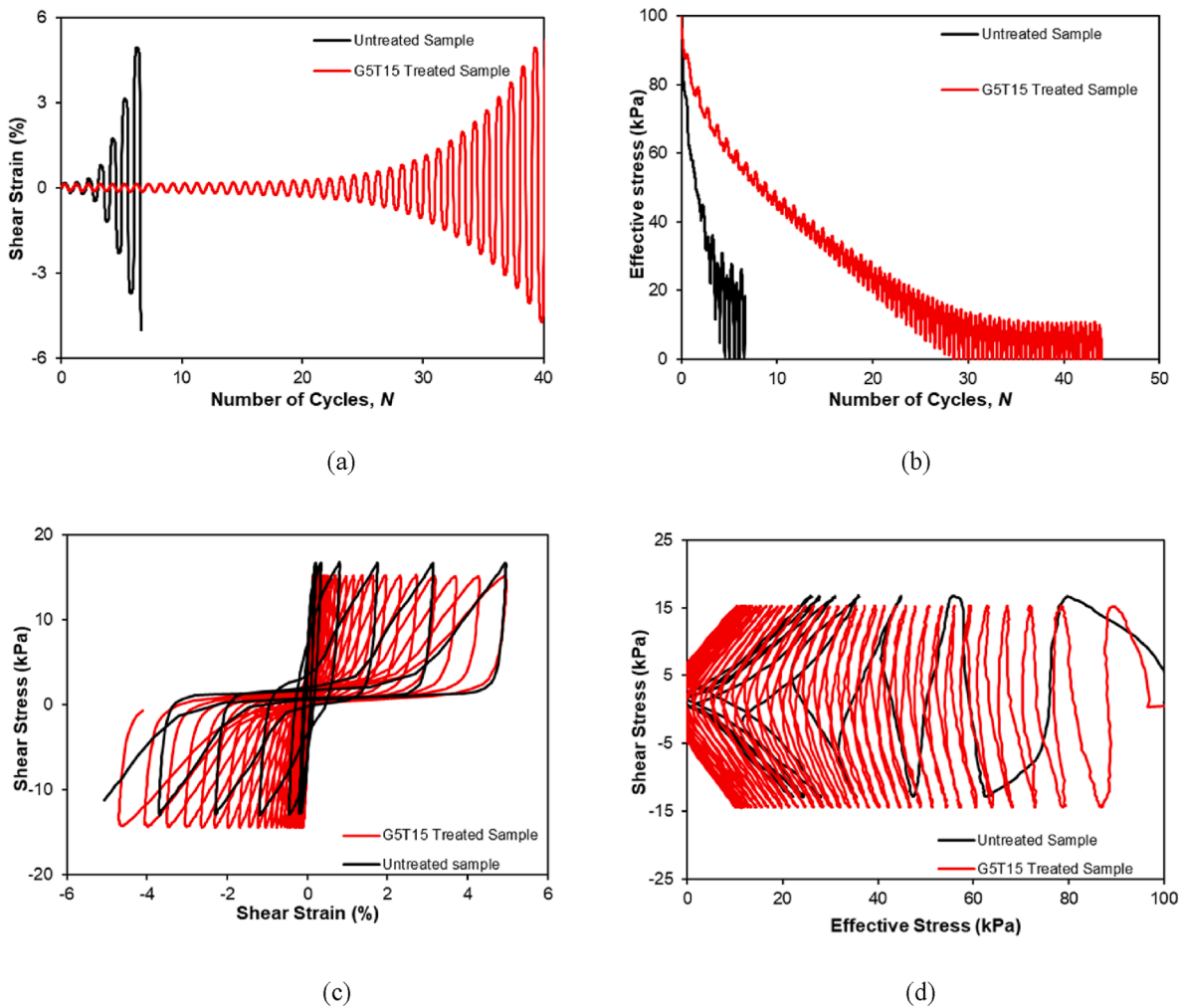


Fig. 18. Cyclic shear test of sub 28 d G5T15-treated and untreated soils (CSR = 0.15).

soil was molded under the same conditions as those used in the previous slake experiment sample production and underwent underwater curing after 7 d of natural drying. The underwater curing periods were 1 d, 7 d, and 28 d. The experimental results indicate that the liquefaction resistance strength was 0.23 after 1 d of underwater curing, 0.20 after 7 d, and 0.19 after 28 d.

Fig. 18 presents the raw data comparing untreated soil and G5T15-treated soil after 28 d of underwater curing, with a CSR of 0.15 applied during cyclic simple shear tests.

Fig. 18a illustrates the relationship between shear strain and the number of cycles. The shear strains for both the G5T15-treated and untreated soils increased with the number of loading cycles.

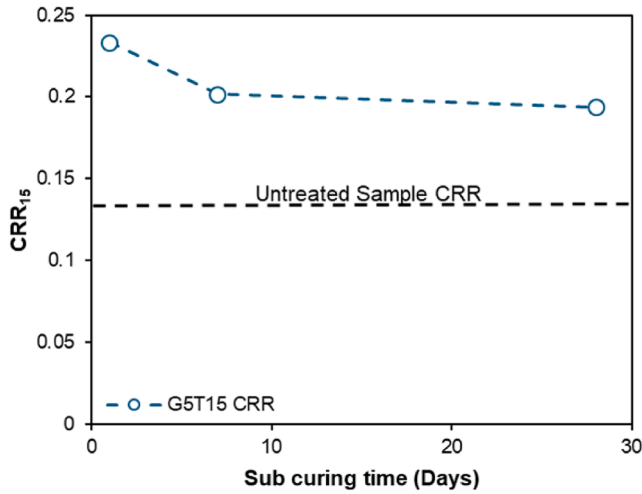


Fig. 19. CRR of treated soil based on underwater curing time.

The untreated soil reached a shear strain of 7.5% after 8 cycles, while the G5T15-treated soil achieved this shear strain after 39 cycles. This indicates that the G5T15-treated soil exhibited higher liquefaction resistance than the untreated soil.

Fig. 18b depicts the relationship between effective stress and the number of repeated loadings. Both the untreated and G5T15-treated soils demonstrated a tendency for effective stress to dissipate as the number of cycles increased. The effective stress of the untreated soil diminished to 0 kPa after 4 or more cycles, whereas the effective stress of the G5T15-treated soil reduced to 0 kPa after 28 or more cycles. This further indicates that the G5T15-treated soil possessed greater liquefaction resistance compared to the untreated soil.

Fig. 18c shows the relationship between shear stress and shear strain. Both the G5T15-treated and untreated soils exhibited an increase in shear strain with applied shear stress. However, it is evident that the untreated soil displayed a larger shear strain than the G5T15-treated soil for the same number of cycles.

Fig. 18d illustrates the relationship between shear stress and effective stress. The untreated soil exhibited a greater degree of effective stress dissipation owing to the cyclic simple shear stress compared to the G5T15-treated soil.

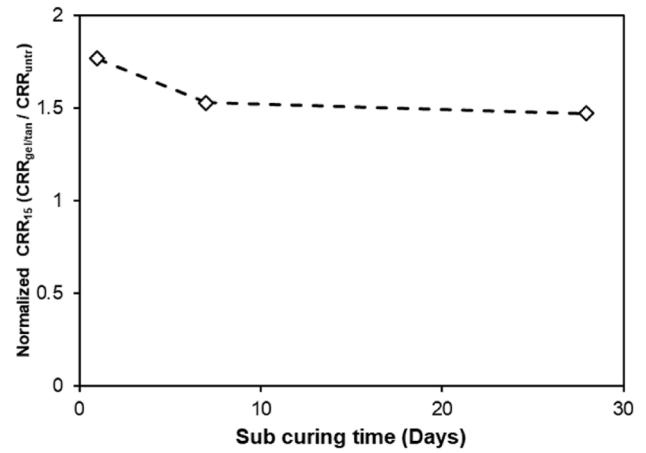


Fig. 21. Normalized CRR<sub>15</sub> based on underwater curing duration.

Fig. 19 depicts the liquefaction resistance strength of G5T15-treated soil according to the number of days of underwater curing. It is evident that the liquefaction resistance strength remains consistently stable up to 28 d of underwater curing when compared to untreated soil.

#### 3.4.2. Cyclic simple shear tests (CRR) analysis

Fig. 20 presents the liquefaction resistance curve for G5T15-treated soil based on the number of underwater curing days. Notably, the liquefaction resistance curve did not show significant changes during the underwater curing period. From this curve, the CSR corresponding to 15 repeated loadings was calculated as CRR<sub>15</sub>, and the liquefaction resistance strength was determined according to the number of underwater curing days. The normalized CRR<sub>15</sub>, obtained by dividing the calculated liquefaction resistance strength by the liquefaction resistance strength of the untreated soil, is illustrated in Fig. 21. The liquefaction resistance strength of the G5T15-treated soil was found to increase by 1.77 times compared to that of the untreated soil on the first day, 1.53 times on the seventh day, and 1.47 times on the 28th day of underwater curing. These results demonstrate that the gelatin–tannic acid-treated soil maintained a stable enhancement in liquefaction resistance strength compared to the untreated soil, even under underwater curing conditions.

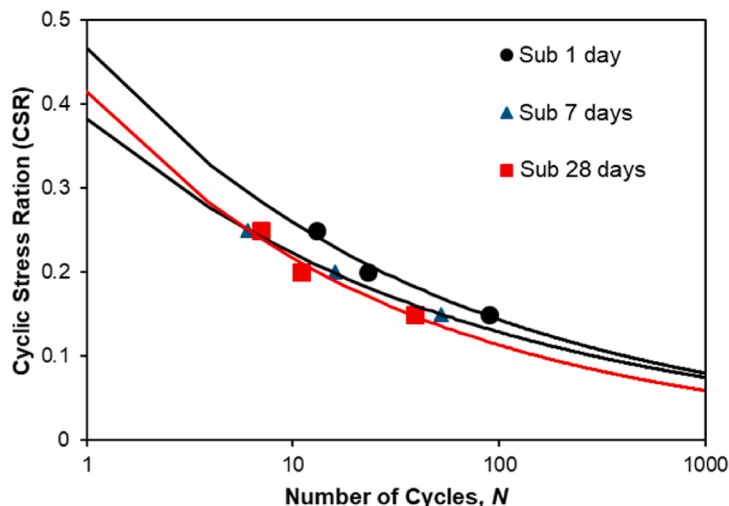


Fig. 20. Liquefaction resistance curve based on underwater curing duration.

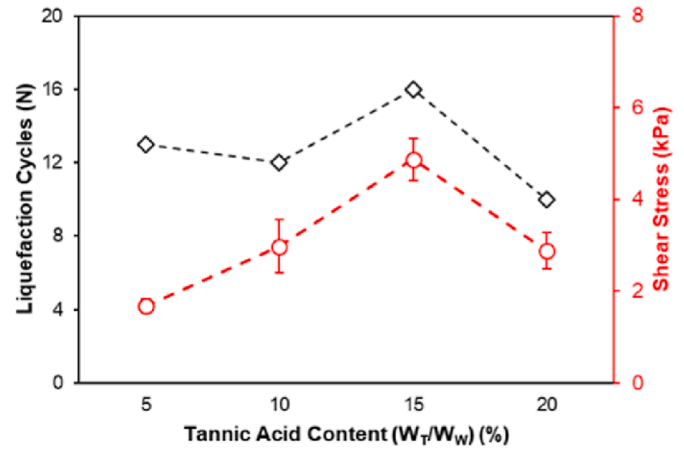
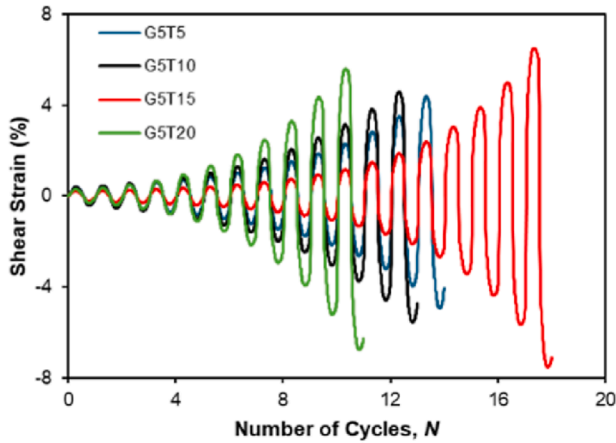


Fig. 22. Shear strength variation with the number of cyclic loading cycles.

The analysis results indicated that the liquefaction resistance strength of the gelatin–tannic acid-treated soil improved even under underwater curing conditions, with the minimum amount of polymer (for economic feasibility) compared to that of the untreated soil. This finding demonstrates that the gelatin–tannic acid-treated soil consistently maintains high liquefaction resistance, even in a long-term underwater environment.

3.4.3. Shear strength of the polymer itself under repeated shear loading

Fig. 22 illustrates the relationship between the number of cycles at which liquefaction occurred and the bonding force of soil particles, taking shearing into account. This was calculated through repeated shear tests following the underwater curing of soil treated with 5%, 10%, 15%, and 20% tannic acid and 5% gelatin. The results confirmed that the bonding force of the soil particles, considering the shearing of the gelatin–tannic acid polymer, correlated consistently with the number of cycles when liquefaction occurred. This indicates that the bonding force, factoring in the shearing of soil particles and polymer, remains effective even under cyclic loading, ensuring that the strength of the treated soil is stably maintained even underwater.

4. Conclusions

In this study, the shear-based bonding strength of gelatin–tannic acid mixed polymers was assessed, along with the underwater durability and liquefaction resistance of gelatin–tannic acid-treated soil through cyclic shear tests. The following conclusions were drawn:

- (1) Tannic acid can form secondary or triple cross-links through hydrogen bonds with molecules that contain hydroxyl and amino groups. Consequently, tannic acid enhances the water resistance of gelatin by inhibiting hydrogen bonding between gelatin molecules and water through its own hydrogen bonds with gelatin.
- (2) Based on the theoretical mechanism of the gelatin–tannic acid reaction, the underwater durability index of the treated soil was assessed through a slake test. The results revealed that the treated soil achieved an underwater durability index close to 100% until the 28th day of underwater curing for all mixing ratios, except G20T5. This confirms that the hydrogen bonds between gelatin and tannic acid effectively enhanced the water resistance of the treated soil.

- (3) Determining the optimal mixing ratio of gelatin–tannic acid based solely on a slake test has its limitations. Therefore, the optimal mixing ratio of gelatin and tannic acid was established through a soil particle bonding experiment that considered shear. The results indicated that the most effective ratio of tannic acid for enhancing mechanical strength through hydrogen bonding when combined with gelatin was 15%.
- (4) The liquefaction resistance strength ( $CRR_{15}$ ) of G5T15-treated soil was evaluated through repeated shear tests under underwater curing conditions. The gelatin–tannic acid-treated soil demonstrated deformation at higher shear stress levels than the untreated soil. Furthermore, the dissipation of effective stress was minimized, leading to increased liquefaction resistance, with stable liquefaction resistance strength maintained until the 28th day of underwater curing. These results indicate that gelatin–tannic acid-treated soil consistently preserves the bonding force between soil particles, even in an underwater curing environment, making it effective in preventing liquefaction.

CRediT authorship contribution statement

**Jeong Youn Lee:** Writing – review & editing, Writing – original draft, Visualization, Validation, Methodology, Investigation, Formal analysis, Data curation, Conceptualization. **Jae-Eun Ryou:** Supervision, Project administration, Investigation, Conceptualization. **Sangbeen Lee:** Visualization, Validation, Software, Methodology. **Beomjoo Yang:** Writing – review & editing, Validation. **Chiyoung Park:** Supervision, Project administration, Methodology. **Jongwon Jung:** Writing – review & editing, Validation, Supervision, Resources, Project administration, Methodology, Formal analysis.

Declaration of competing interest

The authors declare that they have no known competing financial interests or personal relationships that could have appeared to influence the work reported in this paper.

Acknowledgments

This work was supported by a National Research Foundation of Korea (NRF) grant, funded by the Korean government (MSIT) (Grant Nos. 2022R1A4A3029737 and RS-2024-00353644).

## References

- Alshawmar, F., Fall, M., 2021. Dynamic response of thickened tailings in shaking table testing. *Int. J. Geo.Eng.* 12, 1–25.
- ASTM D8296 – 19. Standard Test Method for Consolidated Undrained Cyclic Direct Simple Shear Test under Constant Volume with Load Control or Displacement Control.
- Bolton Seed, H., Tokimatsu, K., Harder, L.F., Chung, R.M., 1985. Influence of SPT procedures in soil liquefaction resistance evaluations. *J. Geotech. Eng.* 111 (12), 1425–1445.
- Chang, I., Im, J., Prasadhi, A.K., Cho, G.C., 2015a. Effects of Xanthan gum biopolymer on soil strengthening. *Constr. Build. Mater.* 74, 65–72.
- Chang, I., Prasadhi, A.K., Im, J., Cho, G.C., 2015b. Soil strengthening using thermo-gelation biopolymers. *Constr. Build. Mater.* 77, 430–438.
- Chang, I., Lee, M., Tran, A.T.P., Lee, S., Kwon, Y.M., Im, J., Cho, G.C., 2020. Review on biopolymer-based soil treatment (BPST) technology in geotechnical engineering practices. *Transp. Geotech.* 24, 100385.
- Chen, C., Wu, L., Perdjon, M., Huang, X., Peng, Y., 2019. The drying effect on xanthan gum biopolymer treated sandy soil shear strength. *Constr. Build. Mater.* 197, 271–279.
- Chen, C., Wei, K., Gu, J., Huang, X., Dai, X., Liu, Q., 2022a. Combined effect of biopolymer and fiber inclusions on unconfined compressive strength of soft soil. *Polymer* 14 (4), 787.
- Chen, C., Yang, H., Yang, X., Ma, Q., 2022b. Tannic acid: a crosslinker leading to versatile functional polymeric networks: a review. *RSC Adv.* 12 (13), 7689–7711.
- Chung, K.T., Zhao, G., Stevens Jr, E., Simco, B.A., Wei, C.I., 1995. Growth inhibition of selected aquatic bacteria by tannic acid and related compounds. *J. Aquat. Anim. Health* 7 (1), 46–49.
- Do, T.M., Laue, J., Mattsson, H., Jia, Q., 2023. Excess pore water pressure generation in fine granular materials under undrained cyclic triaxial loading. *Int. J. Geo. Eng.* 14 (1), 8.
- Fatehi, H., Ong, D.E., Yu, J., Chang, I., 2023. The effects of particle size distribution and moisture variation on mechanical strength of biopolymer-treated soil. *Polymer* 15 (6), 1549.
- Galloway, D.L., Jones, D.R., Ingebritsen, S.E. (Eds.), 1999. *Land Subsidence in the United States*, 1182. U.S. Geol. Surv.
- Gihm, Y.S., Kim, S.W., Ko, K., Choi, J.H., Bae, H., Hong, P.S., et al., 2018. Paleoseismological implications of liquefaction-induced structures caused by the 2017 Pohang earthquake. *Geosci. J.* 22 (6), 871–880.
- González, J.S., Burlaka, A., Paz, J., Salavagione, H.J., Carretero-González, J., Hernández, R., 2020. Compact polyelectrolyte hydrogels of gelatin and chondroitin sulfate as ion's mobile media in sustainable all-solid state electrochemical devices. *Mater. Adv.* 1 (7), 2526–2535.
- Hwang, B., Han, J.T., Kim, J., Kwak, T.Y., 2020. Liquefaction characteristic of Pohang sand based on cyclic triaxial test. *J. Korean Geotech. Soc.* 36 (9), 21–32.
- Iwasaki, T., 1986. Soil liquefaction studies in Japan: state-of-the-art. *Soil Dynam. Earthq. Eng.* 5 (1), 2–68.
- Jafari, H., Ghaffari-Bohlouli, P., Niknezhad, S.V., Abedi, A., Izadifar, Z., Mohammadijad, R., et al., 2022. Tannic acid: a versatile polyphenol for design of biomedical hydrogels. *J. Mater. Chem. B* 10 (31), 5873–5912.
- Jang, C., Yang, B., Hong, W.T., Ahn, J., Jung, J., 2024. Soil improvement using agar gum polymer for seismic liquefaction mitigation. *Soil Dyn. Earthq. Eng.* 177, 108405.
- Jang, C., Yang, B., Hong, W.T., Jung, J., 2025. Evaluation of the static and dynamic behavior characteristics of biopolymer-treated soil at varying moisture contents. *Soil Dyn. Earthq. Eng.* 188, 109080.
- Ji, Y., Kim, B., Kim, K., 2021. Evaluation of liquefaction potentials based on shear wave velocities in Pohang City, South Korea. *Int. J. Geo.Eng.* 12, 1–10.
- Kim, H.S., Kim, M., Baise, L.G., Kim, B., 2021. Local and regional evaluation of liquefaction potential index and liquefaction severity number for liquefaction-induced sand boils in Pohang, South Korea. *Soil Dynam. Earthq. Eng.* 141, 106459.
- Kozlov, P.V., Burdygina, G.I., 1983. The structure and properties of solid gelatin and the principles of their modification. *Polymer* 24 (6), 651–666.
- Lee, S., Ryou, J.E., Kwon, T.H., Jung, J., 2025. Effect of Agar gum on the interparticle bonding and uniaxial compressive strength of soils. *Polym. Test.*, 108828.
- Nagula, S.S., Hwang, Y.W., Dashti, S., Grabe, J., 2021. Seismic site response of layered saturated sand: comparison of finite element simulations with centrifuge test results. *Int. J. Geo.Eng.* 12 (1), 26.
- Naik, S.P., Gwon, O., Park, K., Kim, Y.S., 2020. Land damage mapping and liquefaction potential analysis of soils from the epicentral region of 2017 Pohang Mw 5.4 earthquake, South Korea. *Sustainability* 12 (3), 1234.
- Nong, Z.Z., Park, S.S., Lee, D.E., 2021. Comparison of sand liquefaction in cyclic triaxial and simple shear tests. *Soils Found.* 61 (4), 1071–1085.
- Owen, G., 1987. Deformation processes in unconsolidated sands. *Geol. Soc. London, Spec. Publ.* 29 (1), 11–24.
- Park, S.S., Hwang, S.H., 2012. A study on durability test of cemented soils. *J. Korean Geotech. Soc.* 28 (11), 79–86.
- Park, S.-S., Nong, Z., Choi, S.-G., Moon, H.-D., 2018. Liquefaction resistance of Pohang sand. *J. Korean Geotech. Soc.* 34 (9), 5–17.
- Poppe, J., 1992. *Gelatin. In: Thickening and gelling agents for food*. Springer US, Boston, MA, pp. 98–123.
- Ray, P., Sahu, R.B., 2021. A parametric study on cyclic strength of coastal sand of Digha in West Bengal, India. *Int. J. Geo.Eng.* 12, 1–21.
- Ryou, J.E., Jung, J., 2022. Penetration behavior of biopolymer aqueous solutions considering rheological properties. *Geomech. Eng.* 29 (3), 259–267.
- Ryou, J.E., Jung, J., 2023. Characteristics of thermo-gelation biopolymer solution injection into porous media. *Constr. Build. Mater.* 384, 131451.
- Ryou, J.E., Lee, J.Y., Hong, W.T., Yang, B., Jung, J., 2024a. Effects of curing and soil type on unconfined compressive strengths and hydraulic conductivities of thermo-gelation biopolymer treated soils. *Constr. Build. Mater.* 432, 136493.
- Ryou, J.E., Yang, B., Hong, W.T., Jung, J., 2024b. Pore network approach to evaluate the injection characteristics of biopolymer solution into soil. *Smart Struct. Syst.* 34 (1), 51.
- Sierra, K., An, J., Shamet, R., Chen, J., Kim, Y.J., Nam, B.H., Park, P., 2024. A review of geopolymer binder as a grouting material. *Int. J. Geo.Eng.* 15 (1), 21.
- Sato, C., Haga, M., Nishino, J., 2006. Land subsidence and groundwater management in Tokyo. *Int. Rev. Environ. Strat.* 6 (2), 403–424.
- Schuster, R.L., Fleming, R.W., 1986. Economic losses and fatalities due to landslides. *Bull. Assoc. Eng. Geol.* 23 (1), 11–28.
- Seo, S., Lee, M., Im, J., Kwon, Y.M., Chung, M.K., Cho, G.C., Chang, I., 2021. Site application of biopolymer-based soil treatment (BPST) for slope surface protection: in-situ wet-spraying method and strengthening effect verification. *Constr. Build. Mater.* 307, 124983.
- Smitha, S., Rangaswamy, K., 2020. Effect of biopolymer treatment on pore pressure response and dynamic properties of silty sand. *J. Mater. Civ. Eng.* 32 (8), 04020217.
- Smitha, S., Rangaswamy, K., 2021. Experimental study on unconfined compressive and cyclic triaxial test behavior of agar biopolymer-treated silty sand. *Arabian J. Geosci.* 14, 1–12.
- Smitha, S., Rangaswamy, K., 2022a. Dynamic properties of biopolymer-treated loose silty sand evaluated by cyclic triaxial test. *Test. Evaluation* 50 (1), 315–331.
- Smitha, S., Rangaswamy, K., 2022b. Effect of different parameters on cyclic triaxial response of biopolymer treated soil. *Eur. J. Environ. Civ. Eng.* 26 (15), 7645–7663.
- Soldo, A., Miletic, M., 2022. Durability against wetting-drying cycles of sustainable biopolymer-treated soil. *Polymer* 14 (19), 4247.
- Stevens, J., 1982. Unified soil classification system. *Civ. Eng.* 52 (12), 61–62.
- Teatini, P., Ferronato, M., Gambolati, G., Gonella, M., 2006. Groundwater pumping and land subsidence in the Emilia-Romagna coastland, Italy: modeling the past occurrence and the future trend. *Water Resour. Res.* 42 (1), W01406.
- Vaid, Y.P., Sivathayalan, S., 1996. Static and cyclic liquefaction potential of Fraser Delta sand in simple shear and triaxial tests. *Can. Geotech. J.* 33 (2), 281–289.
- Wang, F., Li, T., 2009. *Landslide Disaster Mitigation in Three Gorges Reservoir*, China. Springer, Berlin, pp. v–ix.
- Worrell, E., Price, L., Martin, N., Hendriks, C., Meida, L.O., 2001. Carbon dioxide emissions from the global cement industry. *Annu. Rev. Energy Environ.* 26 (1), 303–329.
- Xiao, Y., Xiao, W., Wu, H., Zaman, M., 2024a. Tensile strengths and size effects of biocemented sands. *Int. J. GeoMech.* 24 (5), 06024004.
- Xiao, Y., Yan, J., Wu, H., Zaman, M., 2024b. Tensile strength and fracture of interparticle MICP bonds. *Int. J. GeoMech.* 24 (10), 06024019.
- Yakimets, I., Paes, S.S., Wellner, N., Smith, A.C., Wilson, R.H., Mitchell, J.R., 2007. Effect of water content on the structural reorganization and elastic properties of biopolymer films: a comparative study. *Biomacromolecules* 8 (5), 1710–1722.
- Zivari, A., Siavoshnia, M., Rezaei, H., 2023. Effect of lime-rice husk ash on geotechnical properties of loess soil in Golestan province, Iran. *Int. J. Geo.Eng.* 14 (1), 20.



**Jongwon Jung** is a Professor in the School of Civil Engineering at Chungbuk National University. Jongwon Jung received his bachelor's degree and master's degree in civil and environmental engineering from Korea University in 1999 and 2004, respectively. He entered Georgia Tech in 2006 and received his Ph.D. in 2010. After working at Lawrence Berkeley National Laboratory in USA for 1.5 years, he was hired at Louisiana State University in 2012. He moved to Chungbuk National University in 2017. He published more than 84 journal papers (63 international and 21 national).